THE JOURNAL OF BIOLOGICAL CHEMISTRY VOL. 287, NO. 13, pp. 10435–10443, March 23, 2012

Lack of Plakoglobin in Epidermis Leads to Keratoderma*[S]

Received for publication, August 31, 2011, and in revised form, February 6, 2012 Published, JBC Papers in Press, February 7, 2012, DOI 10.1074/jbc.M111.299669

Deqiang Li[‡§], Wenjun Zhang[‡§], Ying Liu[§¶], Laura S. Haneline[§¶], and Weinian Shou[‡§1]

From the [‡]Riley Heart Research Center, [§]Herman B Wells Center for Pediatric Research, Department of Pediatrics, and [¶]Department of Microbiology and Immunology, Indiana University School of Medicine, Indianapolis, Indiana 46202

Background: Plakoglobin (Jup) is involved in intercellular junctions. Mutation of Jup is associated with Naxos disease.
Results: Epidermis-restricted *Jup* knock-outs largely recapitulated human palmoplantar keratoderma. Ultrastructural analyses revealed the disruption of the assembly of desmosomes and adherens junctions in *Jup* mutant epidermis.
Conclusion: Jup is critical for maintaining normal epidermis.
Significance: Our findings provide important insights for the pathogenesis of palmoplantar keratoderma.

Loss-of-function mutation of Jup has been associated with Naxos disease, which is characterized by arrhythmogenic cardiomyopathy and the cutaneous disorder palmoplantar keratoderma. Previously, we have shown that genetic ablation of Jup in cardiomyocytes in mice leads to arrhythmogenic cardiomyopathy similar to Naxos disease in humans. Currently, to determine the pathogenesis of Naxos disease-associated keratoderma, we generated *Jup* mutant mice by inactivating *Jup* restrictively in keratinocytes. *Jup* mutant mice largely recapitulated the clinical features of human palmoplantar keratoderma: overcornification and thickening of the epidermis. *Jup* mutant mice also suffered skin ulceration and inflammation. Cell apoptosis and proliferation were significantly elevated in *Jup* mutant epidermis. Ultrastructural analyses revealed the disruption of the assembly of desmosomes and adherens junctions in *Jup* mutant epidermis. We also demonstrated the compensational increase in β-catenin at *Jup* mutant cell-cell junctions without altering its signaling activities. Our findings provide important insights for understanding the pathogenesis of human palmoplantar keratoderma.

The epidermis, a striated squamous epithelium, acts as the major barrier against pathogens or immunogens from the environment. This is achieved mainly through numerous intercellular junctions between keratinocytes, such as desmosomes, adherens junctions, and tight junctions. Among these junctions, desmosomes provide the primary resistance to the incessant mechanical stresses applied to the epidermis. Epidermal desmosomes bridge between two neighbor cells by homophilic or heterophilic binding of transmembranous desmosomal cadherins (desmoglein and desmocollin) (1). The cytoplasmic tail of desmosomal cadherins interacts with plakoglobin (Jup, also called γ-catenin), which is then associated with the intermediate filament network via desmoplakin. Among these desmosomal proteins, Jup is also a structural component for the adherens junction, in which it is interchangeable with its close homolog, the Armadillo family member β-catenin. Jup and β-catenin share the same degradation machinery and potentially same binding partners (T-cell factor/lymphoid-enhancing factor) in mediating canonical Wnt signaling (2). Thus, Jup has been hypothesized to inhibit canonical Wnt signaling by competing with β-catenin, although this assumption is highly controversial, particularly in terms of different temporal and spatial contexts. Loss-of-function mutation of Jup has been identified in patients with Naxos disease, an autosomal recessive disease characterized by cardiomyopathy and the skin disorder palmoplantar keratoderma (3). Palmoplantar keratoderma is characterized by thick hyperkeratosis over the palms and soles. Interestingly, the deregulation of Wnt signaling has been suggested to play a causal role in the pathogenesis of palmoplantar keratoderma (4), although this suggestion awaits further supporting evidence. In mice, global deletion of Jup results in heart malformations and blister formations on the epidermis (5). However, early embryonic lethality prevents further functional analyses of Jup deletion in postnatal epidermis pathogenesis.

In this study, to better address whether Jup inactivation is sufficient for the emergence of palmoplantar keratoderma and its potential underlying mechanisms, we generated an epidermal conditional knock-out mouse model of *Jup* (*Jup* mutant). These *Jup* mutants largely mimic the human palmoplantar keratoderma condition. We found that cell proliferation, apoptosis, and differentiation are markedly perturbed in *Jup* mutants, likely contributing to the development of keratoderma. Furthermore, we show that *Jup* mutant mice exhibited compromised immune defense, which is likely caused by the loose intercellular junctions between keratinocytes. Ultrastructural analyses revealed abnormal desmosomes and adherens junctions in *Jup* mutant mice. Finally, we demonstrate that there is a compensatory increase in β-catenin at cell-cell junctions, whereas Wnt/β-catenin signaling is unaffected by the loss of *Jup* in keratinocytes.

MATERIALS AND METHODS

Mice—Jup$^{f/f}$ mice were described previously (6). Cytokeratin 14 *K14-Cre* transgenic mice (7) were a gift from Dr. Jingwu Xie (Indiana University, Indianapolis, IN). *fos-lacZ* transgenic mice (8) were purchased from The Jackson Laboratory. All studies

* This work was supported, in whole or in part, by National Institutes of Health Grants HL81092, HL70259, and HL85098 (all to W. S.). This work was also supported by the Riley Children's Foundation (to W. S.).
[S] This article contains supplemental Figs. 1 and 2.
[1] To whom correspondence should be addressed: Herman B Wells Center for Pediatric Research, R4–302D, 1044 W. Walnut, Indianapolis, IN 46202. Tel.: 317-274-8952; E-mail: wshou@iupui.edu.

TABLE 1
Primers used for quantitative RT-PCR analyses

	Forward (5′ → 3′)	Reverse (5′ → 3′)
TNFα	TCTTCTCATTCCTGCTTGTGG	GGTCTGGGCCATAGAACTGA
IL-1β	TGTAATGAAAGACGGCACACC	TCTTCTTTGGGTATTGCTTGG
IL-6	GCTACCAAACTGGATATAATCAGGA	CCAGGTAGCTATGGTACTCCAGAA
Cyclin D_1	GAGATTGTGCCATCCATGC	CTCCTCTTCGCACTTCTGCT
c-*myc*	CCTAGTGCTGCATGAGGAGA	TCTTCCTCATCTTCTTGCTCTTC
c-*fos*	CAGCCTTTCCTACTACCATTCC	ACAGATCTGCGCAAAAGTCC
c-*jun*	CCAGAAGATGGTGTGGTGTTT	CTGACCCTCTCCCCTTGC
GAPDH	TCCTGGTATGACAATGAATACGGC	TCTTGCTCAGTGTCCTTGCTGG

involving the use of mice were in compliance with the National Institutes of Health and were approved by the Indiana University School of Medicine Animal Care and Use Committee.

Quantitative RT-PCR—TRIzol reagent (Invitrogen) was used to extract total RNA from skin. SYBR Green quantitative RT-PCR analyses were performed using the Roche Applied Science LightCycler 480 system. Primers used for quantitative RT-PCR are listed in Table 1.

Immunoblot Analyses—Skin samples were lysed with radioimmune precipitation assay buffer, and proteins were subsequently separated on 4–12% BisTris[2] gels, transferred, and immunoblotted. The following antibodies were used: polyclonal antibody (pAb) against Jup and pan-cadherin and monoclonal antibody (mAb) against α-catenin (Santa Cruz Biotechnology); pAb against β-catenin and β-catenin phosphorylated at Ser-33, Ser-37, and Thr-41 (Cell Signaling Technology); pAb against keratin 5, involucrin, and filaggrin and mAb against keratin 10 (Abcam); pAb against keratin 14 (Covance); mAb against desmogleins 1 and 2 (PROGEN); mAb against Gr-1 (Pharmingen); mAb against E-cadherin (BD Transduction Laboratories); and pAb against ZO-1 (zona occludens-1) (Invitrogen).

Immunofluorescence Staining—Fluorophore-conjugated wheat germ agglutinin and Alexa Fluor-labeled secondary antibodies were from Molecular Probes. Nuclei were stained with DAPI. Photomicrographs were acquired with either a Leica microscope or an Olympus FV1000 confocal microscope using a single exposure time for the same set of sections in each staining.

BrdU Staining and Terminal Deoxynucleotidyltransferase-mediated dUTP Nick End Labeling (TUNEL) Assay—BrdU and TUNEL assays were performed as described previously (9). Briefly, mice were intraperitoneally injected with BrdU labeling reagent (30 mg/kg of body weight) and killed 3–4 h later. The skin was harvested and fixed in 4% paraformaldehyde in PBS overnight. A BrdU labeling and alkaline phosphatase detection kit (Roche Applied Science) was used to detect proliferating cells on paraffin sections from different samples. TUNEL assays were performed on paraffin slides using an ApopTag kit (Chemicon). Eight photographs on average were randomly taken for each sample. The percentage of positively stained cells was quantified using ImageJ software.

Transmission Electron Microscopy—Transmission electron microscopy was performed as described previously (9). Skin samples were fixed in modified Karnovsky's fixative (2% paraformaldehyde and 2% glutaraldehyde in 0.1 M phosphate buffer) at 4 °C overnight.

Statistical Analyses—Results are presented as the mean ± S.E. for parametric data. Student's *t* test was performed for comparison between two groups. A p value of <0.05 was considered significant.

RESULTS

Keratinocyte-restricted Loss of Jup Results in Keratoderma—The cross of $Jup^{f/f}$ and $Jup^{f/+}$/*K14-Cre* mice was expected to give rise to 25% $Jup^{f/f}$/*K14-Cre* (designated *Jup* mutant) offspring. We designated mice with genotypes of $Jup^{f/+}$, $Jup^{f/f}$, and $Jup^{f/+}$/*K14-Cre* as controls in this study because we did not observe skin abnormalities in any of these mice. *Jup* mutant mice appeared normal by the first postnatal week compared with littermate controls (Fig. 1*A*, *panels a–g*). By 2–3 weeks, however, *Jup* mutant mice were significantly smaller than $Jup^{f/f}$ littermate controls and exhibited ulcerations in the skin near joint areas (Fig. 1*B*, *panel a*). All *Jup* mutant mice died before weaning. *Jup* mutant skin was markedly stiffer than $Jup^{f/f}$ littermate control skin. Severe keratoderma was apparent in *Jup* mutant mice through hyperkeratosis in the palms and soles (Fig. 1*B*, *panels b* and *d*). Histology further revealed a marked thickening of *Jup* mutant epidermal layers, including the shedding of the cornified layer and the underlying subcornified layer (granular layer and basal layer), compared with littermate control epidermis (Fig. 1*B*, *panels g* and *h*). In addition, detachment in the granular layer was apparent in *Jup* mutant epidermis. No overt abnormality was found in *Jup* mutant hair follicles.

Inflammation in Jup Mutant Skin—Given the ulcerations seen in *Jup* mutant skin, we suspected that these mice suffered from inflammation. Indeed, we found excessive neutrophil infiltration in *Jup* mutant derma (Fig. 2*A*). Consistently, inflammatory cytokines, including TNFα, IL-1β, and IL-6, were significantly elevated in *Jup* mutant skin (Fig. 2*A*). Furthermore, both the total number and the percentage of peripheral blood neutrophils were significantly higher in *Jup* mutants compared with controls (Fig. 2*B*). Collectively, these data indicate enhanced inflammation in *Jup* mutant mice.

Altered Epidermal Differentiation in Jup Mutant Mice—Because *Jup* mutant epidermal layers were markedly thickened, we next wanted to understand whether or not and how epidermal differentiation was affected. Immunostaining of involucrin, filaggrin, and keratin 10 (suprabasal layer markers) was considerably expanded in *Jup* mutant epidermis compared with control epidermis (Fig. 3*A* and supplemental Fig. 1). The staining of keratin 5 (a basal layer marker) was greatly extended to most of

[2] The abbreviations used are: BisTris, 2-[bis(2-hydroxyethyl)amino]-2-(hydroxymethyl)propane-1,3-diol; pAb, polyclonal antibody; mAb, monoclonal antibody; TUNEL, terminal deoxynucleotidyltransferase-mediated dUTP nick end labeling.

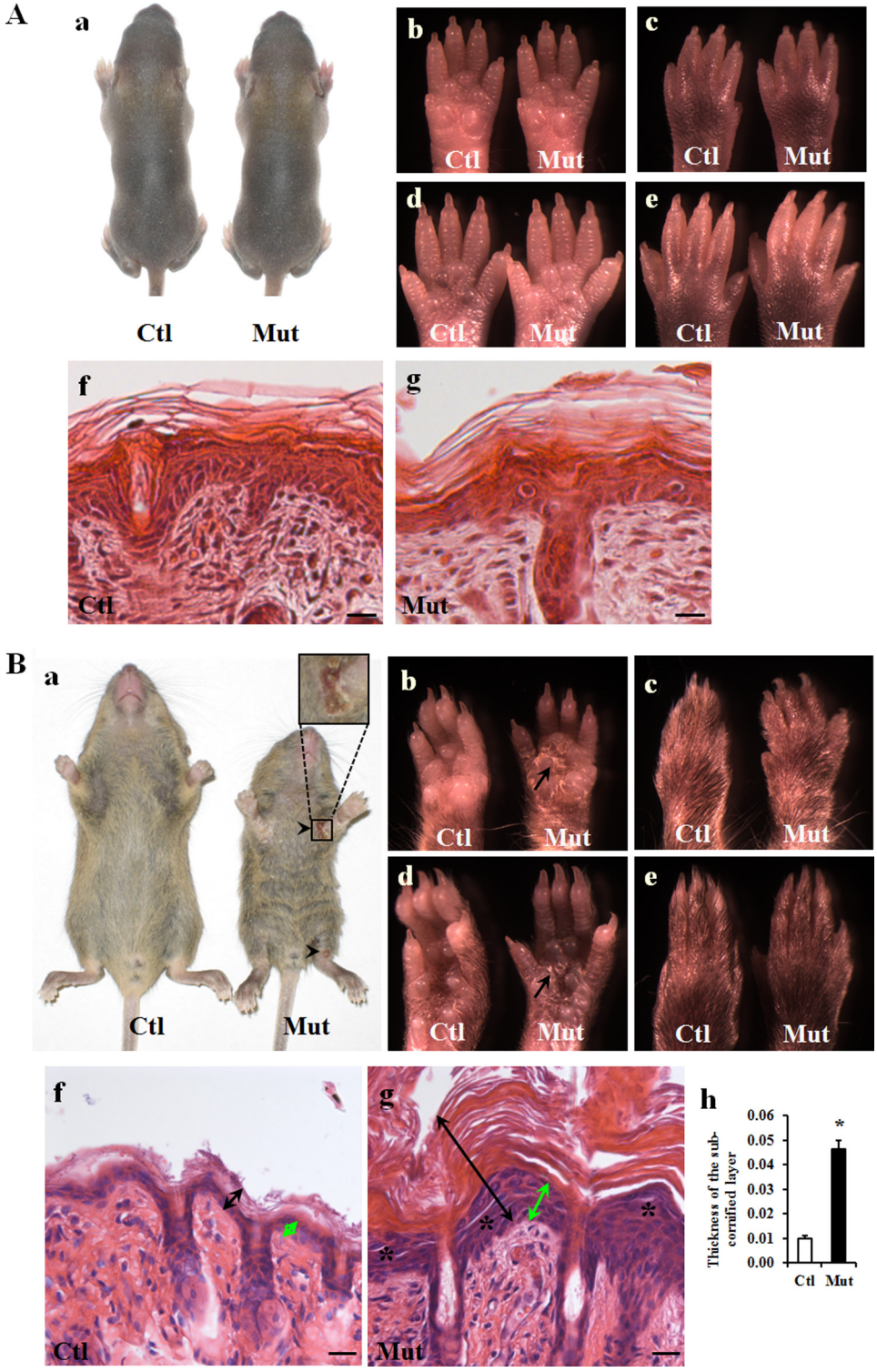

FIGURE 1. **Epidermal phenotypes of *Jup* mutant mice.** *A*, normal epidermis of 1-week-old *Jup* mutant mice. *Panel a*, general morphology of a *Jup* mutant (*Mut*) mouse and a control (*Ctl*) mouse. *Panels b–e*, normal appearance of the *Jup* mutant palm and planta. No apparent plaques are visible. *Panels f* and *g*, normal histology of control and *Jup* mutant epidermis, respectively. *Scale bars* = 20 μm. *B*, *Jup* mutant mice develop an abnormal epidermal phenotype at ~2 weeks after birth. *Panel a*, general morphology of a *Jup* mutant mouse and a control mouse (16 days old). The *Jup* mutant is smaller than its control littermate, and the hair on the *Jup* mutant abdomen is rough. Ulcerations (*arrowheads*) are seen near joint areas. The *Jup* mutant palm exhibits severe hyperkeratosis with plaques (*panel b*, *arrow*), whereas keratosis is mild in the *Jup* mutant planta (*panel d*). No apparent plaques are visible in either the *Jup* mutant opisthenar (*panel c*) or instep (*panel e*). *Jup* mutant epidermis (*panel g*, *double-headed black arrows*) is markedly thicker than control epidermis (*panel f*), with a thick, shedding cornified layer and thickened subcornified layer (*double-headed green arrows*). Detachment of granular layer (*asterisks*) is apparent in *Jup* mutant epidermis. *Scale bars* = 30 μm. Quantitation of the thickness of the subcornified layer is shown in *panel h*. *, significantly different from the control ($p < 0.01$; $n = 4$ (control) and $n = 3$ (mutant)).

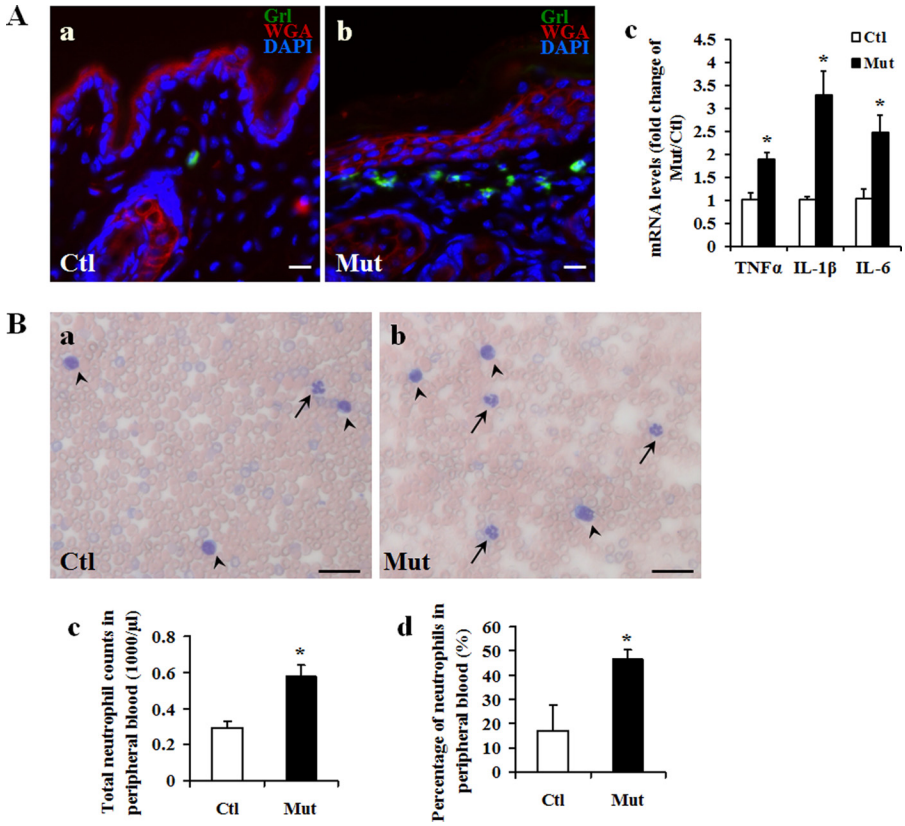

FIGURE 2. **Inflammation in *Jup* mutant skin.** *A*, neutrophil infiltration in *Jup* mutant (*Mut*) derma (16 days old). Note that rare resident neutrophils (Gr-l-positive cells) can be found in the distal control (*Ctl*) derma. *Scale bars* = 20 μm. *WGA*, wheat germ agglutinin. *B*, increase in peripheral blood neutrophils in *Jup* mutants. Representative graphs of Giemsa staining on a peripheral blood smear from *Jup* mutant and control mice (16 days old) are shown in *panels a* and *b*, respectively. *Arrows* and *arrowheads* indicate neutrophils and lymphocytes, respectively. *Scale bars* = 40 μm. HEMAVET analyses in *panels c* and *d* show increased counts and percentage of peripheral blood neutrophils in *Jup* mutants ($n = 7$) compared with controls ($n = 10$). *, $p < 0.001$.

the epidermis with the exception of the cornified layer, which consists of only dead cells without nuclei (Fig. 3*B*). Western blot findings showed increased expression of involucrin and keratin 5 (Fig. 3*C*). These data indicate that epidermal differentiation is remarkably affected by the loss of *Jup* in keratinocytes.

Increased Cell Apoptosis and Proliferation in Jup Mutant Epidermis—Given the development of keratoderma and perturbed epidermal differentiation seen in *Jup* mutant epidermis, we asked whether cell apoptosis or proliferation was affected in *Jup* mutants. First, we found that cell apoptosis was significantly enhanced in *Jup* mutant epidermis as revealed by TUNEL staining (Fig. 4*A*). Notably, the apoptotic cells were located close to the outermost granular layer. Cell proliferation was significantly increased in *Jup* mutant epidermis as assessed by BrdU assay (Fig. 4*B*). Proliferating keratinocytes were confined to the basal layer.

Jup is required for proper cell-cell junctions in the epidermis: Jup is a structural component for both desmosomes and adherens junctions. Although Jup is interchangeable with β-catenin in adherens junctions, only Jup is found in desmosomes under physiological conditions (10, 11). To understand how desmosomes and adherens junctions are affected by Jup deficiency, we first used immunofluorescence staining to demonstrate the specific loss of Jup expression in $Jup^{f/f}$/*K14-Cre* keratinocytes, confirming the successful deletion of *Jup* in keratinocytes (Fig. 5*A*). Next, we assessed the expression of cadherin (specific for adherens junctions), ZO-1 (specific for tight junctions), and desmoglein (specific for desmosomes). The immunostaining intensity of P-cadherin and, more specifically, E-cadherin was similar in both *Jup* mutant and control keratinocytes, although the staining was more expanded in *Jup* mutant epidermis (Fig. 5*B* and supplemental Fig. 2). In contrast, the staining intensity of desmoglein was much stronger in *Jup* mutant keratinocytes compared with control keratinocytes (Fig. 5*B*), in addition to its wider expression in *Jup* mutant epidermis, as seen similarly in the cadherin staining pattern of *Jup* mutant epidermis. ZO-1 staining was also extended in *Jup* mutant epidermis, whereas the staining intensity was similar compared with control epidermis (Fig. 5*C*). Interestingly, the wide-spreading staining of ZO-1 suggests the disturbed cell differentiation in some skin lesions or diseases (12, 13). Thus, this extended ZO-1 staining seen in *Jup* mutant keratinocytes further reinforced the finding of disturbed epidermal differentiation in *Jup* mutants. The results from Western blot analyses of these proteins along with other junctional proteins (α-catenin, specific for adherens junctions; and desmoplakins 1 and 2, specific for desmosomes) were consistent with the results from immunostaining (Fig. 5*D*). To more directly assess the impact of Jup deficiency on cell-cell junctions, ultrastructural analyses by transmission electron microscopy were performed. Wide segregating spaces were seen between adjacent *Jup* mutant keratinocytes (Fig. 5*E*), which was consistent with the histological observation (Fig. 1), indicating cell-cell detachment. Keratin aggregates were often seen in the perinuclear space in *Jup* mutant keratinocytes, but

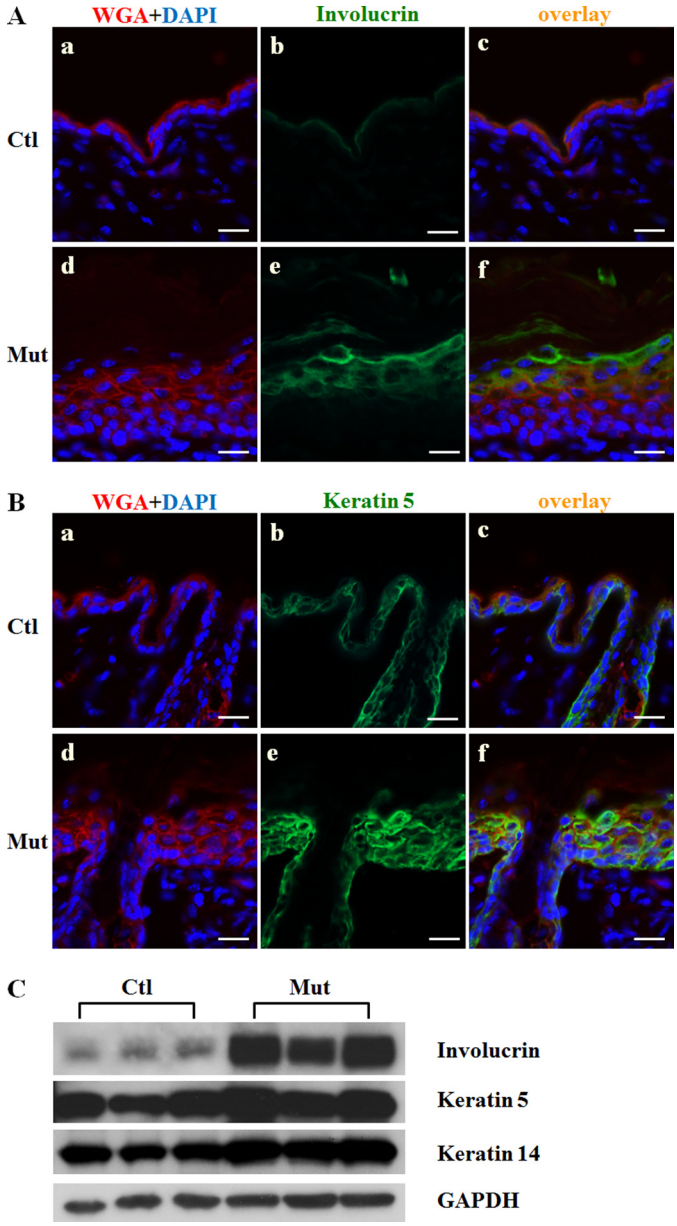

FIGURE 3. **Altered epidermal differentiation of *Jup* mutant mice (16 days old).** *A*, markedly thickened *Jup* mutant (*Mut*) suprabasal layer (*panel e*) compared with the control (*Ctl*; *panel b*) as revealed by involucrin staining. *Scale bars* = 30 μm. *B*, significantly expanded basal layer in *Jup* mutant epidermis (*panel e*) compared with the control (*panel b*) as shown by keratin 5 staining. *Scale bars* = 30 μm. *WGA*, wheat germ agglutinin. *C*, Western blot analyses of involucrin, keratin 5, and keratin 14. GAPDH served as a total protein loading control.

not in control keratinocytes (Fig. 5*E*). Furthermore, atypical desmosomes (the outer plaque of *Jup* mutant desmosomes connected with very few keratin plexuses) were seen in *Jup* mutant keratinocytes (Fig. 5*E*). Adherens junctions in *Jup* mutant keratinocytes displayed abnormally, with wide intercellular spaces. Tight junctions appeared normal in *Jup* mutant epidermis, although abnormal intracellular cell body dissociation was evident in *Jup* mutant keratinocytes (Fig. 5*E*). These intracellular breaks, together with the intercellular gaps in *Jup* mutant epidermis, greatly compromised the competence of the epidermis as a biological barrier. In contrast, hemidesmosomes, in which Jup is known not to be a structural component (14), were still intact in *Jup* mutant keratinocytes (Fig. 5*E*). Collectively, these data suggest that the loss of *Jup* in keratinocytes affects desmosome assembly and compromises the overall integrity of cell-cell junctions, leading to cell-cell detachment.

Increase in β-Catenin at Cell-Cell Junction without Affecting Wnt/β-Catenin Signaling in Jup Mutant Epidermis—Jup has been postulated to have an inhibitory function in Wnt/β-catenin signaling possibly by competing with β-catenin for the same binding partners (2). However, this inhibitory function of Jup in Wnt signaling was still controversial, as shown by existing studies (15, 16). Moreover, the potential influence on Wnt signaling by Jup was considered to be pathogenic (17). Nonetheless, it would be important to determine whether β-catenin and its signaling activities are affected by the loss of *Jup* in keratinocytes. Interestingly, Western blot analyses showed that the total level of β-catenin was overtly increased in *Jup* mutant skin compared with control skin (Fig. 6*A*). A major regulation of the β-catenin level in the cytoplasm is through protein phosphorylation and consequent ubiquitination (18). Phosphorylation of β-catenin at Ser-33, Ser-37, and Thr-41 by glycogen synthase kinase 3β is a primary control for destabilization of β-catenin (19). Using a specific antibody against β-catenin phosphorylated at Ser-33, Ser-37, and Thr-41, we found that phosphorylated β-catenin was markedly reduced in *Jup* mutant skin compared with control skin. This reduction in phosphorylated β-catenin very likely accounts for the increase in total β-catenin. The stabilized β-catenin can either localize to the cell membrane to become a cell-cell junctional constituent or transport into nuclei to behave as a transcriptional activator (20). Immunofluorescence staining revealed that the increase was at the cell membrane, with no detectable signal in the nucleus or cytosol (Fig. 6*B*), thus not suggesting transcriptional activity of β-catenin. To further examine whether the canonical Wnt signaling is altered in *Jup* mutant skin, we analyzed the expression levels of several well known β-catenin transcriptional targets, including cyclin D_1, c-Myc, c-Fos, and c-Jun (21), and found that they were similar between *Jup* mutant and control skin (Fig. 6*C*). To further examine canonical Wnt signaling activities *in vivo*, a specific Wnt/β-catenin signaling reporter mouse line, *fos-lacZ* transgenic mouse (8), was crossed with *Jup* mutant mice. There was no obvious positive X-gal staining signal observed in *Jup* mutant and control epidermis (Fig. 6*D*). In contrast, X-gal staining signals were readily detected in the sebaceous gland and hair roots in both *Jup* mutant and control hair follicles (Fig. 6*D*). These observations were consistent with previous findings (8). The fact that no noticeable difference in staining intensity was found between *Jup* mutants and controls indicates that β-catenin signaling activities are not significantly affected in *Jup* mutant keratinocytes.

DISCUSSION

Keratoderma, a thickening of the stratum corneum of the skin, can be acquired or genetically inherited (22). A homozygous loss-of-function mutation of Jup (Jup2157del2) has been documented in patients with Naxos disease, which manifests cardiomyopathy and palmoplantar keratoderma (3). More recently, several other genetic mutations of Jup have been identified in patients with keratoderma or epidermolysis bullosa

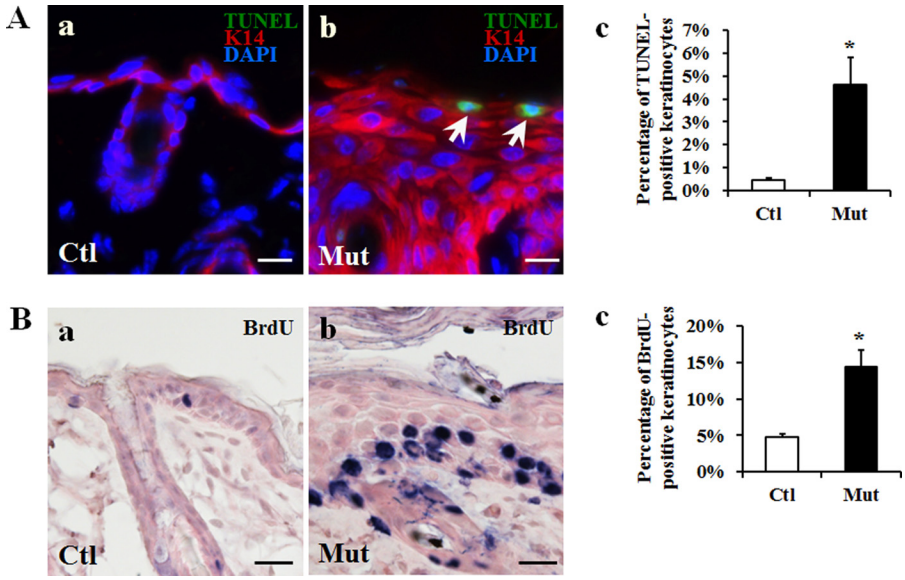

FIGURE 4. **Enhanced cell apoptosis and proliferation in *Jup* mutant epidermis (16 days old).** *A*, TUNEL staining shows increased cell apoptosis in the *Jup* mutant (*Mut*) suprabasal layer (*panel b*) compared with controls (*Ctl*; *panel a*). *White arrows* indicate apoptotic cells. *Scale bars* = 20 μm. *K14*, keratin 14. Quantification is shown in *panel c*. *, $p < 0.001$. *B*, increased cell proliferation in the *Jup* mutant basal layer (*panel b*) compared with controls (*panel a*). The positive BrdU staining is shown as *dark blue* nuclear staining. *Scale bars* = 30 μm. Quantification is shown in *panel c*. *, $p < 0.001$.

(23–25). These Jup mutations lead to either the production of truncated JUP protein or the complete loss of JUP protein. However, the potential underlying mechanisms are not well understood. Herein, we demonstrated that keratinocyte-restricted ablation of *Jup* in mice results in palmoplantar keratoderma.

In this study, we have shown that *Jup* is critical for the cell-cell junctions among keratinocytes. Loss of *Jup* in keratinocytes results in inappropriate desmosome assembly and severe cell-cell detachment. The findings of abnormal formation of desmosomes in *Jup* mutant epidermis are consistent with an early report of global *Jup* knock-out mouse embryos, although the cell-cell detachment phenotype seemed to be much more severe in *Jup* mutant pups (5). The discrepancy is most likely ascribed to the difference in the timing of *Jup* inactivation and the mechanical tension from the surrounding environment: rough cage beddings *versus* amniotic fluid in the uterus. Interestingly, the similar cell-cell dissociation phenotype was also evident in the skin of patients with a homozygous nonsense *JUP* mutation (1615C → T) (24), which further supports the pivotal role of Jup as a cell-cell junction constituent.

The skin inflammation present in *Jup* mutant mice seems contradictory given that *Jup* mutant epidermis was remarkably thickened. However, because *Jup* mutant cell junctions were severely compromised and keratinocytes detached, the skin's function as a defending barrier against innate intruding pathogens is expected to be severely compromised. Indeed, the complication of skin infections was also reported in palmoplantar keratoderma patients (26). All *Jup* mutant mice died before weaning. The following facts likely contributed to the lethality of *Jup* mutants. First, *Jup* mutant skin was thick and stiff, which greatly affected body movement, *e.g.* crawling and suckling. Second, *Jup* mutant skin had ulceration and inflammation accompanied by systemic inflammation as evidenced by the increase in neutrophils in the peripheral blood. The persistent and severe inflammation undoubtedly lessened their survival chance.

The relationship between Jup and β-catenin has been controversial (2). Our data demonstrate that β-catenin was increased at the plasma membrane to compensate for the loss of Jup at cell-cell junctions. Our results are consistent with some early findings of the ectopic localization of β-catenin in *Jup*-deficient desmosomes (10, 27). Nonetheless, β-catenin appears to incompetently substitute for *Jup* at cell junctions because *Jup* mutant cell junctions are loose; consequently, cells detach and undergo apoptosis. As a response, *Jup* mutant epidermis accelerates cell proliferation and differentiation in an attempt to further compensate for the loss of upper layer keratinocytes. Future work will be to analyze the underlying molecular signaling mechanism for the compensatory increase in keratinocyte proliferation associated with *Jup* deficiency. Interestingly, the increase in β-catenin in *Jup* mutant epidermis is specific to cell junctions without affecting Wnt/β-catenin signaling activities, which was clearly evidenced by the lack of nuclear localization of β-catenin, the unaffected levels of its transcriptional targets, and undisturbed T-cell factor/lymphoid-enhancing factor signaling reporter activities. This finding is consistent with our previous observation in cardiomyocyte-restricted *Jup* knock-out mutant mice: a compensational increase in β-catenin at junctions with no effect on its signaling activities (28). Thus, our findings do not suggest that the disturbance of Wnt/β-catenin signaling activities contributes to the pathogenesis of Jup-related keratoderma.

In summary, *Jup* mutant mice recapitulate the pathophysiological features of human palmoplantar keratoderma. We found that *Jup* is critical for maintaining the integrity of intercellular junctions and cell differentiation and proliferation. Additionally, we demonstrated the increase in β-catenin at cell junctions in compensation for the loss of Jup without affecting its signaling activities. Our current findings have provided

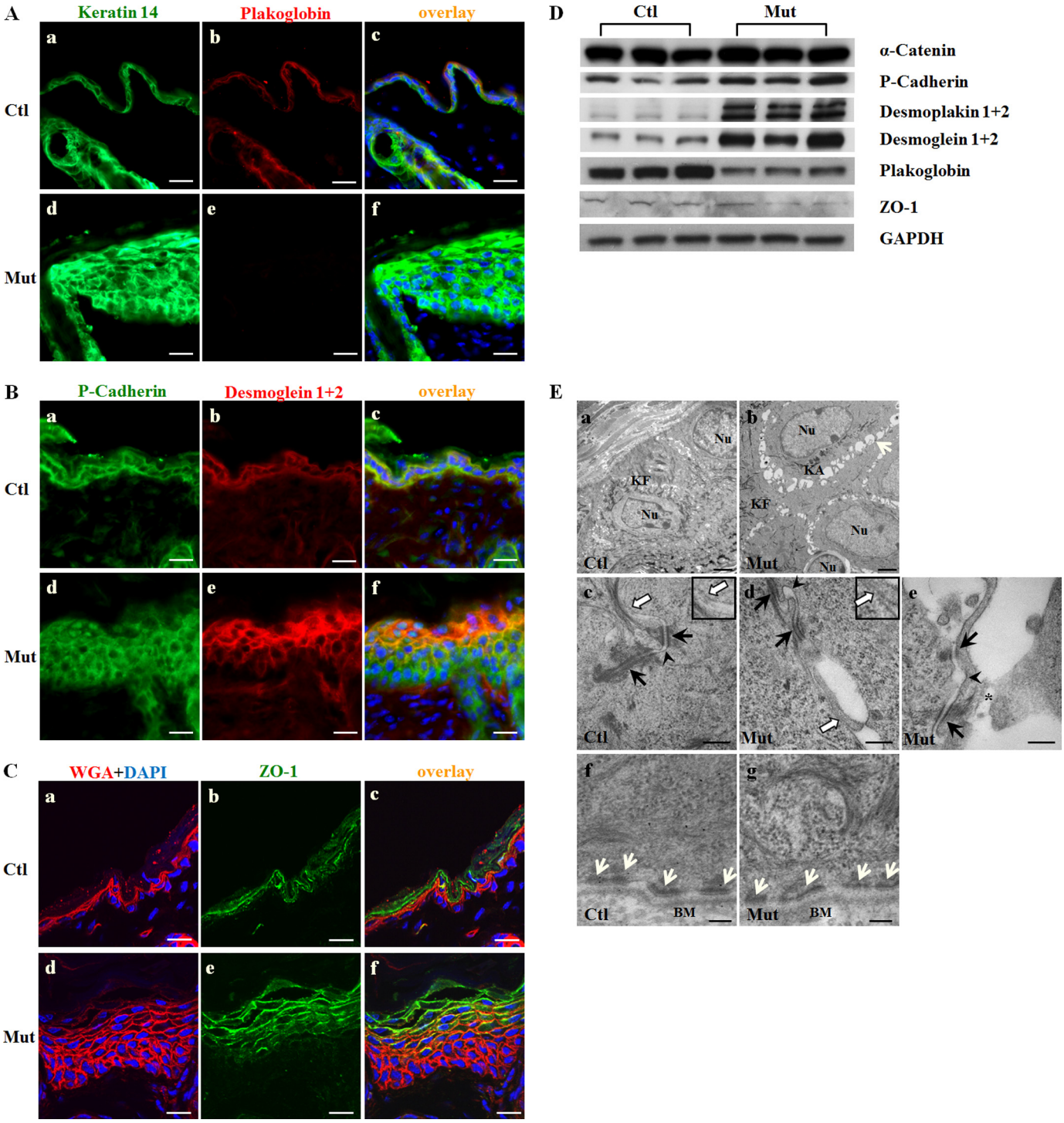

FIGURE 5. **Assessment of cell-cell junction in *Jup* mutant epidermis.** *A*, plakoglobin staining signal was lost in *Jup* mutant (*Mut*) keratinocytes (*panel e*) as opposed to membranous localization in control (*Ctl*) cells (*panel b*), whereas keratin 14 staining intensity was markedly increased in *Jup* mutant cells (*panel d*) compared with control cells (*panel a*). *Panels c* and *f*, overlay images. *Scale bars* = 30 μm. *B*, P-cadherin staining was similar between *Jup* mutant (*panel d*) and control (*panel a*) epidermis. Staining of desmogleins 1 and 2 was greatly increased in *Jup* mutant epidermis (*panel e*) compared with the control (*panel b*). *Scale bars* = 30 μm. *C*, the staining intensity of ZO-1 was similar between *Jup* mutant (*panel e*) and control (*panel b*) epidermis, although the signal was much expanded in *Jup* mutant epidermis. *WGA*, wheat germ agglutinin. *Scale bars* = 15 μm. *D*, Western blot analyses of cell junction proteins. *E*, ultrastructural analyses of *Jup* mutant epidermis. Loose cell-cell contacts between *Jup* mutant keratinocytes (*panel b*) are shown by segregated spaces (*white arrows*). Keratin fibers (*KF*) are at cell peripheries in both control (*panel a*) and Jup mutant (*panel b*) keratinocytes. Keratin aggregates (*KA*) are seen in the perinuclear (*Nu*) region of *Jup* mutant keratinocytes (*panel b*), but not in control cells (*panel a*). Desmosomes (*black arrows*) are anchored to the keratin plexus in control keratinocytes (*panel c*), whereas significantly fewer keratins are at *Jup* mutant desmosomes (*panels d* and *e*). The intercellular spaces of adherens junctions (*arrowheads*) are wider in *Jup* mutant keratinocytes (*panels d* and *e*) than in control keratinocytes (*panel c*). Tight junctions (*white arrows*) appear normal in *Jup* mutant keratinocytes (*panel d*). Tight junctions are also presented at higher magnification in the *insets* in *panels c* and *d*. Note that the partial cell membrane and associated cytoplasm (*asterisk*) are disintegrated from the *Jup* mutant keratinocyte cell body (*panel e*). In contrast, hemidesmosomes (*white arrows*) are intact in *Jup* mutant keratinocytes (*panel g*). *BM*, basal membranes. *Scale bars* = 2 μm (*panels a* and *b*), 250 nm (*panels c–e*), and 125 nm (*panels f* and *g*).

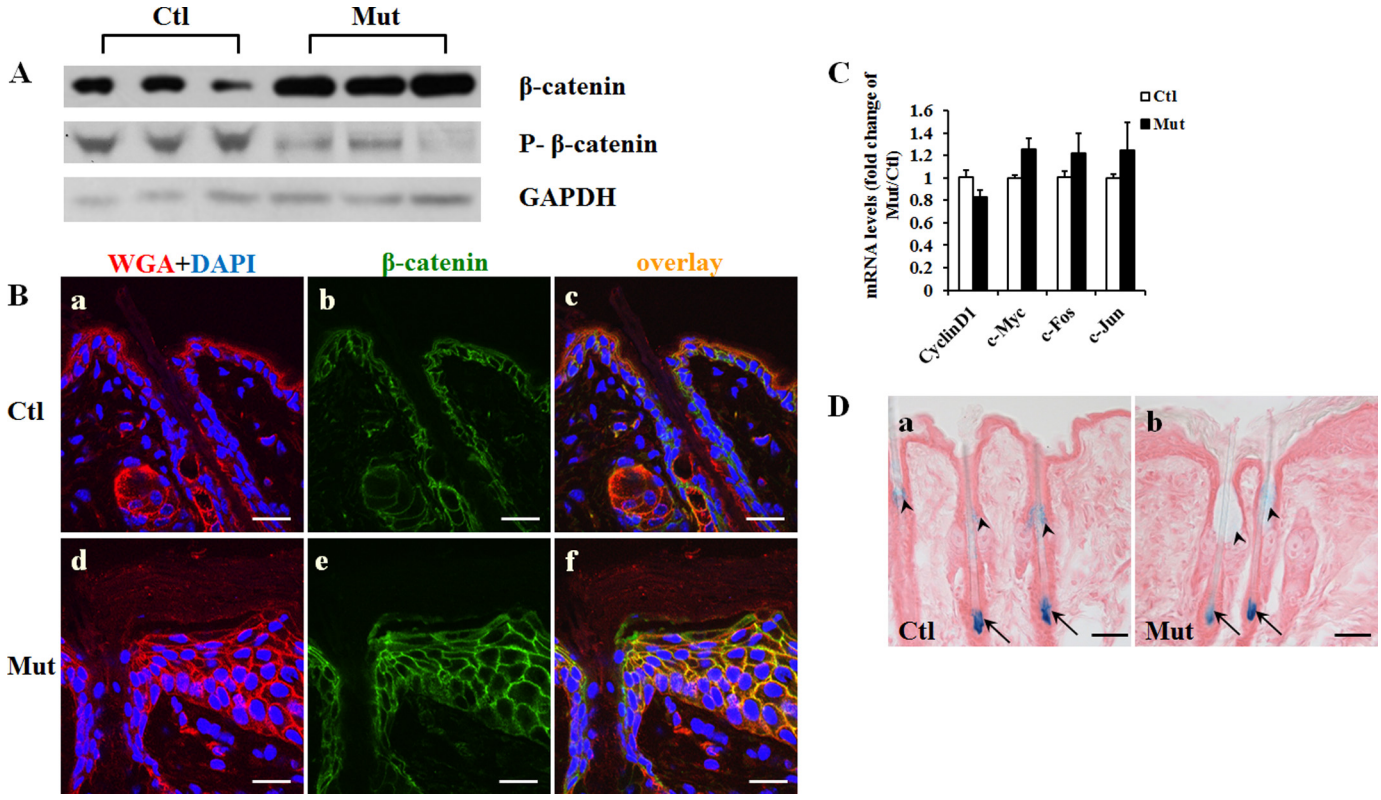

FIGURE 6. **Increase in β-catenin at cell membrane in *Jup* mutant epidermis.** *A*, Western blot of total β-catenin and β-catenin phosphorylated at Ser-33, Ser-37, and Thr-41. *B*, representative confocal photographs of β-catenin in 16-day-old *Jup* mutant (*Mut*) and control (*Ctl*) epidermis. The expression of β-catenin at the membrane of *Jup* mutant keratinocytes was markedly increased compared with the control keratinocyte membrane. The signal was undetectable in the nuclei or cytosol in either *Jup* mutant or control keratinocytes. *Scale bars* = 20 μm. *WGA*, wheat germ agglutinin. *C*, assessment of Wnt/β-catenin signaling targets by quantitative RT-PCR. There was no statistical difference between controls ($n = 3$) and *Jup* mutants ($n = 3$). *D*, representative pictures of X-gal staining of $Jup^{f/f}$/*fos-lacZ* epidermis (*panel a*) and $Jup^{f/f}$/*K14-Cre/fos-lacZ* skin (*panel b*). There was no positive signal in the epidermis of either controls (*panel a*) or *Jup* mutants (*panel b*). X-Gal staining signals were readily detected in the sebaceous gland region (*arrowheads*) and hair roots (*arrows*) in both *Jup* mutant and control hair follicles. No overt difference in staining intensity was found between *Jup* mutants and controls. *Scale bars* = 50 μm.

important insights for understanding the pathogenesis of keratoderma.

Acknowledgments—We thank Dr. Jingwu Xie for generously providing K14-Cre mice and Dr. Mark H. Kaplan (Indiana University, Indianapolis) for anti-involucrin and anti-filaggrin antibodies. We thank Dr. Mark Soonpaa (Indiana University, Indianapolis) for critical reading of the manuscript.

REFERENCES

1. Jamora, C., and Fuchs, E. (2002) Intercellular adhesion, signaling, and the cytoskeleton. *Nat. Cell Biol.* **4,** E101–E108
2. Zhurinsky, J., Shtutman, M., and Ben-Ze'ev, A. (2000) Plakoglobin and β-catenin: protein interactions, regulation, and biological roles. *J. Cell Sci.* **113,** 3127–3139
3. McKoy, G., Protonotarios, N., Crosby, A., Tsatsopoulou, A., Anastasakis, A., Coonar, A., Norman, M., Baboonian, C., Jeffery, S., and McKenna, W. J. (2000) Identification of a deletion in plakoglobin in arrhythmogenic right ventricular cardiomyopathy with palmoplantar keratoderma and woolly hair (Naxos disease). *Lancet* **355,** 2119–2124
4. Van Steensel, M. A. (2010) Recessive palmoplantar keratodermas: a tale of wings, hands, hair. and cancer. *G. Ital. Dermatol. Venereol.* **145,** 763–770
5. Bierkamp, C., Mclaughlin, K. J., Schwarz, H., Huber, O., and Kemler, R. (1996) Embryonic heart and skin defects in mice lacking plakoglobin. *Dev. Biol.* **180,** 780–785
6. Li, D., Liu, Y., Maruyama, M., Zhu, W., Chen, H., Zhang, W., Reuter, S., Lin, S. F., Haneline, L. S., Field, L. J., Chen, P. S., and Shou, W. (2011) Restrictive loss of plakoglobin in cardiomyocytes leads to arrhythmogenic cardiomyopathy. *Hum. Mol. Genet.* **20,** 4582–4596
7. Jonkers, J., Meuwissen, R., van der Gulden, H., Peterse, H., van der Valk, M., and Berns, A. (2001) Synergistic tumor suppressor activity of BRCA2 and p53 in a conditional mouse model for breast cancer. *Nat. Genet.* **29,** 418–425
8. DasGupta, R., and Fuchs, E. (1999) Multiple roles for activated LEF/TCF transcription complexes during hair follicle development and differentiation. *Development* **126,** 4557–4568
9. Li, D., Hallett, M. A., Zhu, W., Rubart, M., Liu, Y., Yang, Z., Chen, H., Haneline, L. S., Chan, R. J., Schwartz, R. J., Field, L. J., Atkinson, S. J., and Shou, W. (2011) Dishevelled-associated activator of morphogenesis 1 (Daam1) is required for heart morphogenesis. *Development* **138,** 303–315
10. Acehan, D., Petzold, C., Gumper, I., Sabatini, D. D., Müller, E. J., Cowin, P., and Stokes, D. L. (2008) Plakoglobin is required for effective intermediate filament anchorage to desmosomes. *J. Invest. Dermatol.* **128,** 2665–2675
11. Fukunaga, Y., Liu, H., Shimizu, M., Komiya, S., Kawasuji, M., and Nagafuchi, A. (2005) Defining the roles of β-catenin and plakoglobin in cell-cell adhesion: isolation of β-catenin/plakoglobin-deficient F9 cells. *Cell Struct. Funct.* **30,** 25–34
12. Pummi, K., Malminen, M., Aho, H., Karvonen, S. L., Peltonen, J., and Peltonen, S. (2001) Epidermal tight junctions: ZO-1 and occludin are expressed in mature, developing, and affected skin and *in vitro* differentiating keratinocytes. *J. Invest. Dermatol.* **117,** 1050–1058
13. Malminen, M., Koivukangas, V., Peltonen, J., Karvonen, S. L., Oikarinen, A., and Peltonen, S. (2003) Immunohistological distribution of the tight junction components ZO-1 and occludin in regenerating human epidermis. *Br. J. Dermatol.* **149,** 255–260
14. Tsuruta, D., Hashimoto, T., Hamill, K. J., and Jones, J. C. (2011) Hemidesmosomes and focal contact proteins: functions and cross-talk in keratinocytes, bullous diseases, and wound healing. *J. Dermatol. Sci.* **62,** 1–7

15. Klymkowsky, M. W., Williams, B. O., Barish, G. D., Varmus, H. E., and Vourgourakis, Y. E. (1999) Membrane-anchored plakoglobins have multiple mechanisms of action in Wnt signaling. *Mol. Biol. Cell* **10,** 3151–3169
16. Shimizu, M., Fukunaga, Y., Ikenouchi, J., and Nagafuchi, A. (2008) Defining the roles of β-catenin and plakoglobin in LEF/T-cell factor-dependent transcription using β-catenin/plakoglobin-null F9 cells. *Mol. Cell. Biol.* **28,** 825–835
17. Garcia-Gras, E., Lombardi, R., Giocondo, M. J., Willerson, J. T., Schneider, M. D., Khoury, D. S., and Marian, A. J. (2006) Suppression of canonical Wnt/β-catenin signaling by nuclear plakoglobin recapitulates phenotype of arrhythmogenic right ventricular cardiomyopathy. *J. Clin. Invest.* **116,** 2012–2021
18. Clevers, H. (2006) Wnt/β-catenin signaling in development and disease. *Cell* **127,** 469–480
19. Yost, C., Torres, M., Miller, J. R., Huang, E., Kimelman, D., and Moon, R. T. (1996) The axis-inducing activity, stability, and subcellular distribution of β-catenin are regulated in *Xenopus* embryos by glycogen synthase kinase 3. *Genes Dev.* **10,** 1443–1454
20. Haq, S., Michael, A., Andreucci, M., Bhattacharya, K., Dotto, P., Walters, B., Woodgett, J., Kilter, H., and Force, T. (2003) Stabilization of β-catenin by a Wnt-independent mechanism regulates cardiomyocyte growth. *Proc. Natl. Acad. Sci. U.S.A.* **100,** 4610–4615
21. MacDonald, B. T., Tamai, K., and He, X. (2009) Wnt/β-catenin signaling: components, mechanisms, and diseases. *Dev. Cell* **17,** 9–26
22. Itin, P. H., and Fistarol, S. K. (2005) Palmoplantar keratodermas. *Clin. Dermatol.* **23,** 15–22
23. Cabral, R. M., Liu, L., Hogan, C., Dopping-Hepenstal, P. J., Winik, B. C., Asial, R. A., Dobson, R., Mein, C. A., Baselaga, P. A., Mellerio, J. E., Nanda, A., Boente Mdel, C., Kelsell, D. P., McGrath, J. A., and South, A. P. (2010) Homozygous mutations in the 5′ region of the *JUP* gene result in cutaneous disease but normal heart development in children. *J. Invest. Dermat.* **130,** 1543–1550
24. Pigors, M., Kiritsi, D., Krümpelmann, S., Wagner, N., He, Y., Podda, M., Kohlhase, J., Hausser, I., Bruckner-Tuderman, L., and Has, C. (2011) Lack of plakoglobin leads to lethal congenital epidermolysis bullosa: a novel clinico-genetic entity. *Hum. Mol. Genet.* **20,** 1811–1819
25. Erken, H., Yariz, K. O., Duman, D., Kaya, C. T., Sayin, T., Heper, A. O., and Tekin, M. (2011) Cardiomyopathy with alopecia and palmoplantar keratoderma (CAPK) is caused by a *JUP* mutation. *Br. J. Dermatol.* **165,** 917–921
26. Gamborg Nielsen, P. (1984) Psoriasis and hereditary palmoplantar keratoderma complicated with a dermatophyte infection. Case report. *Dermatologica* **168,** 293–295
27. Bierkamp, C., Schwarz, H., Huber, O., and Kemler, R. (1999) Desmosomal localization of β-catenin in the skin of plakoglobin-null mutant mice. *Development* **126,** 371–381
28. Li, D., Liu, Y., Maruyama, M., Zhu, W., Chen, H., Zhang, W., Reuter, S., Lin, S. F., Haneline, L. S., Field, L. J., Chen, P. S., and Shou, W. (2011) Restrictive loss of plakoglobin in cardiomyocytes leads to arrhythmogenic cardiomyopathy. *Hum. Mol. Genet.* **20,** 4582–4596